Optical, electrical and electrochemical properties of heteroaromatic copolymers

John P. Ferraris and Thomas R. Hanlon
Programs in Chemistry, The University of Texas at Dallas, Richardson, Texas 75083-0688, USA
(Received 19 July 1988; revised 28 November 1988; accepted 6 December 1988)

Three-ring monomers based on α-terthienyl in which the heteroatom of the central ring is varied between S, O, N or N–CH_3 were electropolymerized to produce films on either transparent conducting electrodes or Pt. The former were characterized by *in situ* Vis/n.i.r. absorption spectroscopy as a function of oxidation level, and as free-standing films by *FT*i.r. and four-probe d.c. electrical conductivity measurements. The latter were characterized by cyclic voltammetry. The effect of heteroatom composition and film growth conditions on the redox and optical properties of the copolymers is discussed. A qualitative energy level diagram for the copolymers is presented.

(Keywords: thiophene–pyrrole copolymers; thiophene–furan copolymers; thiophene–*N*-methylpyrrole copolymers; electropolymerization; Vis/n.i.r. absorption spectroscopy; cyclic voltammetry; conductivity)

INTRODUCTION

Polymers based on heteroaromatic molecules have received considerable attention recently due to their interesting electrical, optical and electrochemical properties[1]. Many of these studies have been motivated by the promise these systems offer as useful electronic materials and devices and reports have appeared describing the use of conducting polymers in field-effect transistors[2], as electrode materials for battery applications[3], in heterojunction solar cells with inorganic semiconductors[4,5], in p–n junction diodes with other conducting polymers[6], in Schottky barrier junctions[7], in molecule-based transistors[8], in electrically conducting composites[9–12] and membranes[13], for information storage[14], as fast response non-linear optical materials[15], and as humidity sensors[16].

The properties of these materials are variable over a wide range of conductivity, processibility, and stability depending on the type (number) of substituents, ring fusions, etc., present in the monomer (and presumably the resultant polymer). One variable that is expected to be important is the heteroatom composition. We have reported[17] a series of copolymers of thiophene with pyrrole, *N*-substituted pyrroles, furan and selenophene, in which there is a controlled S/X (X = NH, N–R, O or Se) ratio in the copolymer and a formally known sequence distribution. These 'substitutional alloys' were prepared in powder form by chemical oxidation of the appropriate three ring system, shown in *Figure 1*, where the heteroatom of the central ring, X, is varied between NH [SNS, *1*), N–CH_3 [SMS, *2*], O [SOS, *3*] and S [SSS, *4*].

Four-probe d.c. conductivity measurements on compressed pellets suggested that the heteroatom composition did influence the magnitude of the conductivity for comparably doped SXS polymers but due to the high overall doping levels (21–49 mole %) of the systems studied, we were unable to determine the sensitivity of the conductivity to this variable. The work reported here, which focuses on the 'alloys' prepared in thin film form by electrochemical polymerization, has enabled further elucidation of the importance of this variable.

TRANSPORT AND OPTICAL PROPERTIES OF POLY(HETEROAROMATICS)

The electrical properties of the poly(heteroaromatics) can be varied from insulating to highly conducting upon chemical (electrochemical) oxidation and reduction. Marked electrochromism often accompanies these changes. Although the term 'doping' has been applied to the process of oxidation–reduction in these materials, it is not the same phenomenon that occurs with traditional inorganic semiconductors like Si or GaAs, because the polymeric systems are typically 'doped' to the tenths-to-several per cent levels, resulting in salt structures. Transport occurs in the polymer subsystem. The counterions serve primarily to maintain electroneutrality.

The poly(heteroaromatics) may assume the two bonding arrangements, benzenoid and quinoid, displayed as the structures within the brackets in *Figure 2*, (I) and (II), respectively. The carbon framework of the benzenoid phase resembles a polyacetylene (PA) in which there are four-carbon all-*trans* units linked by a *cis*-like structure and is more stable than the quinoid phase, which has more *cis*-linkages[18]. Although the energy difference between the two phases will not be as large in polyheteroaromatics as it is for the *trans* and *cis* polyacetylene isomers, this lack of degeneracy nevertheless precludes the stable soliton structures which are observed for PA[18]. The oxidation (or reduction) of the benzenoid poly(heteroaromatic) chain is accompanied by a structural transformation to the quinoid form and changes in its absorption spectra. Removal (addition) of a single electron results in the formation of a *p*-type (n-type) radical ion (called a polaron) with the associated energy

0032-3861/89/071319-09$03.00

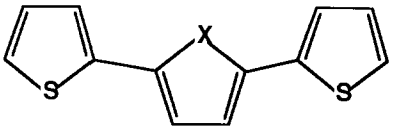

X = NH	SNS	1
X = NMe	SMS	2
X = O	SOS	3
X = S	SSS	4

Figure 1 Structures of and acronyms for tri-ring monomers

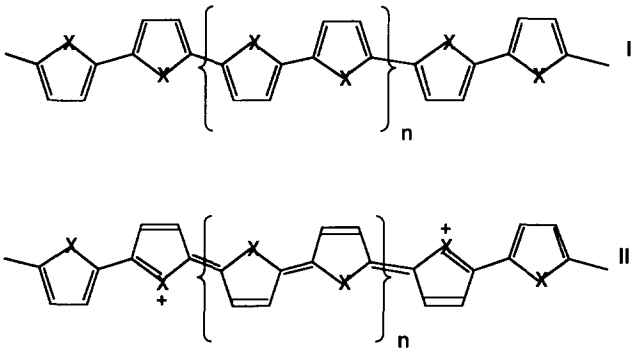

Figure 2 Two possible bonding arrangements for poly(heteroaromatics). The benzenoid and quinoid phases are given in the brackets of structures I and II, respectively

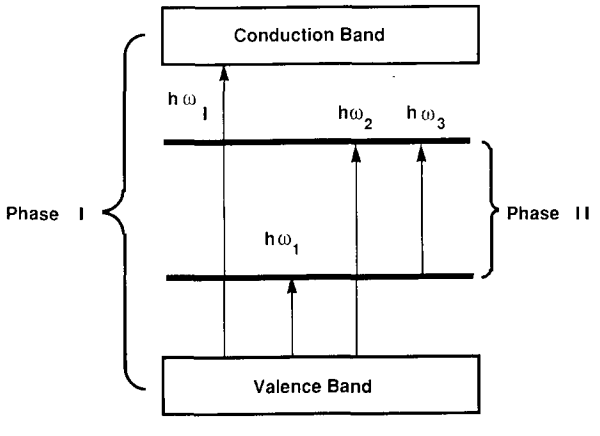

Figure 3 Energy level diagram for benzenoid (Phase I) and quinoid (Phase II) for poly(heteroaromatics). The widths of the valence and conduction bands are arbitrary. See text for explanation of optical transitions $h\omega_I$ and $h\omega_{1-3}$

level diagram of *Figure 3*. The quinoid phase possesses a lower ionization potential and higher electron affinity than the benzenoid phase[19] so its HOMO and LUMO lie in the midgap region of the benzenoid phase.

For *p*-type polarons the lower mid-gap state is singly occupied; for n-type, this lower state is filled and the upper mid-gap state is singly occupied. As the 'doping' level increases, the radical portions of multiple polarons appearing on the same chain can combine into pi-bonds leaving behind bipolarons (di-ions) which straddle 'quinoidal' segments (*Figure 2* (II), shown for the *p*-type bipolaron). The bipolaron upper and lower states are either both empty or both doubly occupied for *p*-type or n-type materials, respectively. Optical transitions from the valence band to the bonding polaron (bipolaron) level $[h\omega_1]$, or to the antibonding polaron (bipolaron) level $[h\omega_2]$ or to the conduction band $[h\omega_I]$ are allowed[18]. An additional transition between the singly occupied lower polaron level and its upper level $[h\omega_3]$ has also been observed in lightly oxidized polypyrrole[20]. This absorption is absent in more highly doped polypyrrole where the polaron bonding state has been replaced by an unoccupied bipolaron state and at all doping levels of polythiophene[18]. It has been suggested that the kinetics of polaron pair recombination is faster in polythiophene than in polypyrrole due to the greater degree of order in the former[21].

The evolution of the energy level diagram as a function of doping for the heteroaromatic polymers will depend on a number of factors including the ease with which a particular ring achieves the quinoidal arrangement (a function of the nature of heteroatom (X) in as much as it affects the 'aromaticity' of the various heteroaromatics); the degree to which the various X atoms contribute to the HOMO (not significantly different for the various heteroatoms, to a first approximation) and LUMO (significantly different for the various heteroatoms) levels, in so far as the band gaps in the solid may be related to these molecular levels; and steric effects which may inhibit adjacent rings in Phase II from achieving coplanarity. This last factor will decrease the mobility of bipolarons[20] which will be reflected in the electrical properties of the polymer. The SXS polymers of *Figure 1* allow us to address several of these factors.

EXPERIMENTAL

General

All reagents and solvents were ACS reagent grade unless otherwise specified. Solvents were distilled from the appropriate drying agent prior to use. Water content was monitored using a Photovolt Aquatest IV Karl Fischer titrator. Infra-red spectra were obtained on a Nicolet 5DX *FT*i.r. and absorption spectra were obtained on either a Hewlett–Packard HP-8450A (UV/Vis) or Hitachi EPS-3T UV/Vis/NIR Spectrophotometer which was interfaced via a 12 bit ADC (Applied Engineering, Inc.) to an Apple IIe microcomputer. The synthesis and characterization of the SXS monomers *1–4* has been described previously[17]. Four probe conductivity measurements were made with a T-909 Resistivity Test Set (Self-Organizing Systems, Inc.), at room temperature.

Electrochemical polymerizations

All solution preparation and polymerizations were conducted in a Vacuum Atmospheres Inc. glove box filled with high purity helium. The solution concentrations ranged from 0.02–0.10 M monomer, with 0.10 to 0.50 M supporting electrolyte. The best electrolyte/solvent systems consisted of $LiClO_4$ with 1-methyl-2-pyrrolidinone (NMP distilled from CaH_2), propylene carbonate (PC distilled from CaH_2) or tetrahydrofuran (THF distilled from $LiAlH_4$). Other supporting electrolytes that were examined included tetrabutylammonium hexafluorophosphate (TBAHFP), tetrabutylammonium tetrafluoroborate (TBATFB), tetra-

ethylammonium *p*-toluenesulphonate (TEAOTs), and lithium *p*-toluenesulphonate (LiOTs). Other solvents included acetonitrile (MeCN, distilled from CaH_2), *N*,*N*-dimethylformamide (DMF, distilled from CaH_2) and dimethylsulphoxide (DMSO, dried over molecular sieves). All electrochemical polymerizations were effected using an EG&G PARC Model 173 Potentiostat. The films were grown on indium–tin oxide (ITO) coated glass slides which were precut to 1 cm widths. These were positioned parallel to an Al plate counter electrode of similar dimensions held 3 mm away. This sandwich was placed in a one compartment cell which also held a Ag wire that served as a pseudo reference electrode. Most polymerizations were carried out at constant potential, resulting in current densities that varied between 0.5 and 5.3 mA/cm^3 (for different runs) which dropped during the reaction between 5–30%. In cases where polymerizations were conducted under constant current (always $\leqslant$6 mA/cm^2) the monitored potential would also drop during the polymerization, usually by less than 20% from its initial value. With $LiClO_4$ electrolyte, as the monomer oxidatively polymerizes, Li^+ ions are reduced and alloy with the Al counter electrode, presumably contributing no cathodic products to the solution and allowing a one compartment cell to be used with impunity. As the polymerization proceeds, the solution often darkens due to 'bleeding' of the reaction products from the electrode. The degree to which this occurs depends on the particular monomer, solvent, growth potential and electrolyte. Under ideal conditions, films grow uniformly on the electrode surface after 30–90 s. These were transparent to visible light. Longer growth periods resulted in films that were no longer transparent, although still uniform, or, in some cases, films that thickened as powdery deposits.

Cyclic voltammetry

Cyclic voltammetric experiments used this same potentiostat coupled to an EG&G PARC Model 175 programmer. A three compartment cell was used. The working electrode consisted of a Pt disc (100 mm diameter) separated by a frit from a carbon counter electrode. The reference electrode consisted of a silver wire suspended in the electrolyte solution (0.5 M $LiClO_4$ in PC) which was saturated with $AgNO_3$. This was separated from the electrolysis compartment by a 3 mm length of unfused Vycor. The voltammograms were collected on a Houston Model 2000 recorder or a Nicolet 2090 digital oscilloscope which was interfaced to a Zenith Model 159 microcomputer (IEEE 488) for data analysis using commercially available software (Waveform Basic, Blue Feather Software, Inc.).

Spectroelectrochemistry

Thin films ($\approx$5 μm) grown on ITO electrodes were positioned as the anode in an electrochemical doping cell. A Pt wire to which a strip of Li was affixed served as both the counter and pseudo reference electrode. The Li ribbon was scraped clean before use. The cell was filled with electrolyte ($LiClO_4$ in PC) and sealed in the glove box. It was then removed and placed in the sample beam of the u.v./vis./n.i.r. spectrophotometer. A cuvette containing electrolyte and a clean ITO electrode was placed in the reference beam. The potential of the film was adjusted (vs Li) with an EG&G PARC Model 173 potentiostat. A typical doping/dedoping experiment involved 15–30 voltage settings with a spectrum taken after each potential step. Equilibration times between steps were typically $\approx$20–30 min or until there was no measured current change in the cell.

RESULTS AND DISCUSSION

Film growth

Table 1 summarizes the film growth conditions that were surveyed in this work. Details of selected film growths follow.

Poly(SSS) films. The best films of poly(SSS) were grown by applying a constant potential ranging (in different experiments) between 1.8 to 3.9 V across the cell. Corresponding current densities ranged between 0.5 to 3 mA/cm^2. Removal of the electrode after 2–4 min revealed a thin, smooth blue-green film. Longer growth periods afforded thicker films. The polymerization is not 'clean' in that the growth solutions became progressively darker with time as soluble products (oligomers?) bled away from the electrode surface. Films could be removed from the electrode by pressing transparent tape against them (a technique employed to obtain samples for conductivity measurements) or by floating them off in aqueous ammonia. The latter procedure also reduced the polymers to their neutral state. After rinsing with ethanol and drying under vacuum, these films were examined by

Table 1 Electropolymerization conditions for SXS monomers

Monomer (molarity)	Growth/ doping solvent	Electrolyte (molarity)	Voltage[d] or current/cm^2	Results[a]
SSS (0.1)	NMP/na	$LiClO_4$ (0.1)	2.4 mA	r,s,NG
SSS (0.1)	NMP/na	TEAOTs (0.1)	1.2 mA	r,s,NG
SSS (0.1)	NMP/NMP[c]	$LiClO_4$ (0.5)	0.7–1.9 mA	f,NG
SSS (0.1)	PC/PC	$LiClO_4$ (0.5)	1.8–3.9 V	r,s,NG
SSS (0.1)[b]	NMP/PC[b]	$LiClO_4$ (0.5)[b]	1.8–3.9 V[b]	f,g[b]
SPS (0.1)	NMP/na	TBAHFP (0.1)	1.1–4.5 mA	r,s,NG
SOS (0.1)	NMP/NMP[c]	LiOTs (0.1)	1.6–3.5 mA	f,NG
SOS (0.1)	NMP/na	$LiClO_4$ (0.5)	2.25 mA	r,NG
SOS (0.1)	NMP/na	$LiClO_4$ (0.5)	1.1 mA	n,NG
SOS (0.08)	NMP/na	$LiClO_4$ (0.5)	2.8 V	r,NG
SOS (0.1)	PC/PC	$LiClO_4$ (0.5)	2.0–3.5 V	f,d,l,NG
SOS (0.05)	PC:NMP/PC	$LiClO_4$ (0.5)	2.0–3.5 V	f,d,p,G
SOS (0.1–0.025)[b]	PC/THF[b]	$LiClO_4$ (0.5)[b]	2.0–3.5 V[b]	f,g,l,G[b]
SNS (0.08)	NMP/na	TBAHFP (0.1)	1.5 mA	s,NG
SNS (0.03)	MeCN/na	TBAHFP (0.1)	0.75 mA	n,NG
SNS (0.02)	MeCN/na	TBAHFP (0.1)	1.85–2.7 V	f,p,NG
SNS (0.1)	NMP/NMP[c]	TEAOTs (0.1)	1.2–2.0 mA	s,r,NG
SNS (0.1)	NMP/na	$LiClO_4$ (0.5)	2.0–2.9 V	vs,NG
SNS (0.1)	PC/PC	$LiClO_4$ (0.5)	1.0–2.7 V	f,d,NG
SNS (0.1)	PC:NMP/PC	$LiClO_4$ (0.5)	1.0–2.7 V	f,d,NG
SNS (0.02)	THF/THF	$LiClO_4$ (0.1)	2.7 V	f,l,G
SNS (0.02)	THF/PC	$LiClO_4$ (0.5)	2.7 V	f,l,NG
SNS (0.1)	PC/THF	$LiClO_4$ (0.5)	1.25–2.7 V	f,d,l,G
SNS (0.025)[b]	PC/PC[b]	$LiClO_4$ (0.5)[b]	1.25–2.7 V[b]	f,l,G[b]
SMS (0.1)	NMP/na	$LiClO_4$ (0.1)	2.0–3.5 mA	r,s,NG
SMS (0.1)	NMP/na	TEAOTs (0.1)	1.5–2.0 mA	r,p,s,NG
SMS (0.1)	PC/na	$LiClO_4$ (0.5)	6.0 mA	r,p,s,NG
SMS (0.08)	PC:NMP/PC	$LiClO_4$ (0.35)	2.5 V	f,r,NG
SMS (0.08)[b]	PC/PC[b]	$LiClO_4$ (0.5)[b]	1.8–3.9 V[b]	f,G[b]

[a] na, not applicable; f/n, film/no film; l, leaching problem (see text); d, film dissolves (see text); p, powdery deposit; r, rough, mottled surface; s, spotty, uneven surface; v, very; G/NG, good/poor growth system
[b] System used for *in situ* spectroelectrochemical work
[c] Unacceptable for doping use
[d] Growth potentials are referenced to a Ag wire pseudo-reference electrode

*FT*i.r. Poly(SSS) films were best prepared in NMP but the potential window of this solvent was inappropriate for doping studies. The polymer-coated ITO electrodes were rinsed copiously in PC and placed in the doping cell with electrolyte and a Li-clad Pt reference/counter electrode. Occasionally the dark colour of the 'as grown' films would fade to a reddish tinge (implying reduction) but the samples would quickly recover their blue-green colour upon application of a slight oxidizing potential. Also, during the course of doping/dedoping cycle (typically an 8–15 h experiment) some soluble fractions leached into the electrolyte solution. This problem could be alleviated, however, by holding a freshly prepared film at oxidizing potentials between 3.7–4.0 V vs Li in fresh electrolyte for 10–30 min prior to the *in situ* doping/dedoping experiments. This suggests that the soluble fractions that are entrained in the film are either polymerized or expelled from the film. This 'pretreatment' procedure was routinely applied to all films. The samples were placed in fresh electrolyte and sealed in the doping cell. *Figure 4* displays the absorption spectrum for a poly(SSS) film as a function of doping between 3.2 and 4.2 V vs Li (0.2–1.2 V vs SCE). The spectra are plotted as their difference from the neutral polymer[18]. This mode of representation facilitates the extraction of the band gap (taken as the point of zero crossing of the x axis). Films can be cycled reversibly between these two extremes. Subjecting the films to more positive potentials resulted in irreversible spectral changes. The maximum 'allowable' potential, determined empirically for each type of poly(SXS) film, was the one above which irreversible spectral changes occurred.

At the lowest potential, the film is in its neutral state and the π–π^* transition appears with a peak around 2.73 eV. As the applied potential is stepped up, this peak decreases in intensity and blue shifts while two additional transitions grow in at lower energies. This general trend has been observed for other heteroaromatic polymers and is taken as the signature of (bi)polarons[18]. *Figure 5* shows the energy shifts for these three peaks for one poly(SSS)

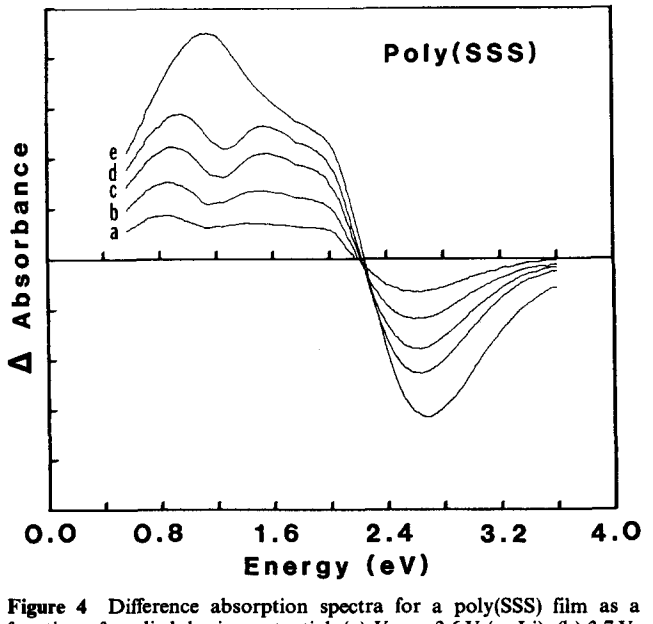

Figure 4 Difference absorption spectra for a poly(SSS) film as a function of applied doping potential. (a) $V_{appl} = 3.6$ V (vs Li); (b) 3.7 V; (c) 3.8 V; (d) 3.9 V; (e) 4.2 V. All spectra are referenced to the neutral polymer produced at $V_{appl} = 3.2$ V (vs Li)

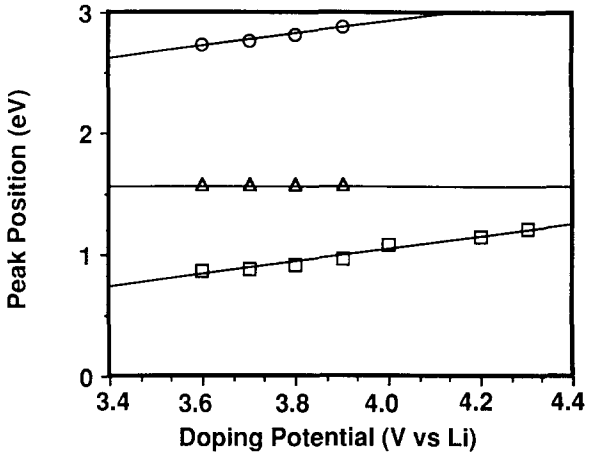

Figure 5 Peak position (eV) vs applied doping potential for a poly(SSS) film. ○, $h\omega_I$; □, $h\omega_1$; △, $h\omega_2$

sample as a function of the doping potential. The peak maxima corresponding to the $h\omega_I$ and $h\omega_1$ transitions blue shift at similar rates as the doping level is increased, whereas the energy of transition $h\omega_2$ remains essentially constant. Films grown at different potentials (current densities) display similar behaviour in this spectral region but manifest differences in the infra-red.

Poly(SOS) films. The preparation of poly(SOS) films proved more troublesome. Films of suitable thickness for the optical studies were prepared from solutions containing 0.025–0.1 M SOS and 0.5 M $LiClO_4$ in PC at applied potentials (currents) between 2.0 and 3.5 V (0.6–2.2 mA/cm^2) but these rapidly dissolved in the growth solution once the potential was removed or when rinsed with pure PC. Some relief was obtained by rapidly removing the ITO electrode from the growth solution and rinsing with THF. The 'pretreatment' procedure described above was particularly necessary for poly(SOS) films which seem to incorporate substantial quantities of soluble material. Multiple THF rinsings and cycling of the film in THF/$LiClO_4$ electrolyte produced films which were stable to the *in situ* doping conditions. It is known that polymers of this type incorporate solvent with the dopant ion[22]. It is thought that several doping/dedoping cycles might result in either further polymerization of SOS oligomers and/or replacement of incorporated PC by THF. The latter might also serve to rinse out any soluble SOS fractions. The exact role played by the incorporated solvent in governing the polymer's characteristics is not known but it is possible that different solvents swell the polymers to different extents thus influencing the mobility of ions/small neutral molecules into the polymer's matrix. The empirically determined maximum potential to which poly(SOS) films could be reversibly oxidized was 4.15 V vs Li. The films were cycled between 3.2 and 4.0 V vs Li for the absorption measurements.

Poly(SNS) films. SNS could be electropolymerized with many different combinations of solvents and electrolyte over a range of applied potentials (or currents). Films grew rapidly in PC but also rapidly dissolved off the ITO electrode when the applied potential was removed. Films of sufficient insolubility for optical measurements were grown from 0.025 M solutions of SNS in PC at applied potentials > 1.25 V (vs Ag). Some soluble material eluted

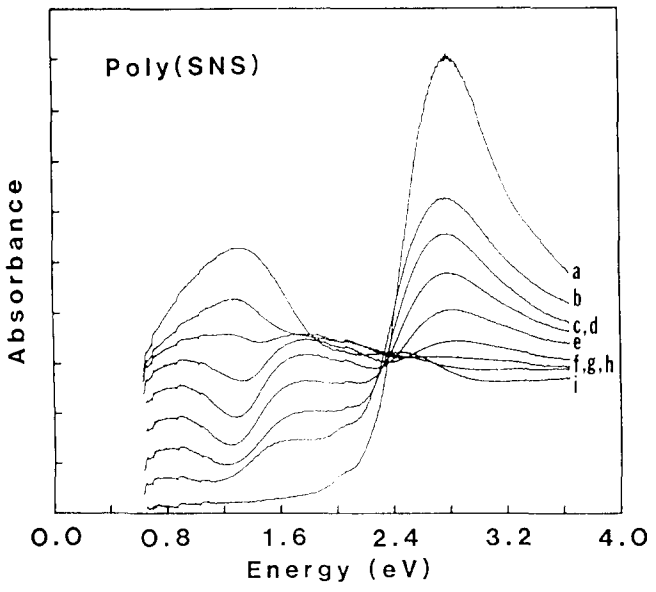

Figure 6 Absorption spectra for *in situ* doping of a poly(SNS) film as a function of applied doping potential. (a) $V_{appl} = 3.0$ V (vs Li); (b) 3.1 V; (c) 3.2 V; (d) 3.3 V; (e) 3.4 V; (f) 3.5 V; (g) 3.6 V; (h) 3.7 V; (i) 4.0 V

into the wash and 'pretreatment' solvents and these were examined by u.v./Vis spectroscopy. Besides ν_{max} of the monomer (340 nm), several peaks at longer wavelength were observed. Of these, the strongest one occurred at 430 nm, close to the π–π^* transition observed for the neutral poly(SNS) films (477 nm). Longer wavelength peaks were also observed, but these were weak. After multiple rinses, the bleeding of these soluble fractions ceased. Poly(SNS) films could be reversibly cycled between 1.8 and 4.1 V vs Li but spectral features at potentials between 1.8 to 2.8 V were identical A representative set of absorption spectra from *in situ* doping of poly(SNS) is given in *Figure 6*.

Poly(SMS) films. Poly(SMS) films grew readily from 0.1 M solutions of the monomer in PC containing 0.5 M $LiClO_4$. An applied potential of 2.2 V for one minute produced a uniform green film. The methyl substituent on the pyrrole significantly changes several characteristics of the polymer. The as-grown films do not release any detectable soluble fractions upon rinsing or even after an extended doping cycle. Poly(SMS) films are less prone to cracking than similarly prepared poly(SNS) films and retain their colour and conductivity even after months of exposure to the atmosphere. Highly oxidized poly(SMS) films are dark blue-grey to black. Partially oxidized films are green and neutral ones are a light yellow-orange. *In situ* absorption spectra for poly(SMS) films were obtained between 2.5 and 4.1 V vs Li. Like the other SXS polymers, the absorption due to the π–π^* transition of the neutral polymer blue shifts and decreases in intensity as the material is oxidized.

FT*i.r. measurements.* It is known that non-α linkages in the polyheteroaromatics can have deleterious effects on the electrical properties of the materials because they increase the band gaps and decrease the band widths[23,24]. Conflicting literature reports on poly(S), poly(SS) and poly(SSS) conclude that the number of rings in the starting monomer used in electrochemical oxidative polymerization increases[25] or decreases[26] the effective degree of conjugation in the resulting polythiophene. Polymerization of SSS monomers occurs at lower potentials than SS or S, reflecting the greater stability (and increased selectivity?) of the radical cation. Furthermore, because this monomer already has three rings α-linked, the resultant polymer is expected to be more linear. On the other hand, others[26] have pointed out that the β-positions become more susceptible to coupling as the length of the monomer chain increases.

Consider the C–H out of plane bending modes for thiophene (S), 2,2′-bithiophene (SS) and α-terthienyl (SSS) monomers. The absorptions for the α-hydrogens occur in the 675–715 cm^{-1} region, cleanly separated from those for the β-hydrogens which occur at 833 cm^{-1} for thiophene[27] and over the range 817–835 cm^{-1} for SS and SSS, with an additional peak for SSS corresponding to the β″-hydrogens of the central ring appearing at 798 cm^{-1} (see *Figure 7*).

Polymerization to yield a totally α-linked polymer should result in a strong absorbance in the vicinity of 800 cm^{-1}, i.e. due to the β″-hydrogens of thiophene rings flanked by thiophene rings, and much weaker absorbances appearing at higher frequency due to the β- and β′-hydrogens of the end groups. The ratios of these two absorbances varies depending on the degree of polymerization (d.p.) and the per cent of mislinked rings. Assuming that the two peaks corresponding to the (β+β′)-hydrogens of the end-groups and the β″-hydrogens of internal thiophene moieties can be resolved, their calculated ratio as a function of the degree of polymerization for 0%, 50% and 100% mislinked polymer will exhibit the behaviour displayed in *Figure 8*.

Electropolymerization of SSS at 1.8 V results in a sharp decrease in the absorption for the α-hydrogens and a collapse of the β-region into a strong absorption around 790 cm^{-1} with a weaker feature near 840 cm^{-1}. As the growth potential of the polymer is increased, however, the relative area of the latter peak also increases with respect to the former. Without knowing d.p. it is not possible to uniquely determine the degree of mislinking in the polymers but estimates of the upper limit of this coupling mode may be inferred from the normalized relative areas of the two absorption regions. We find that for SSS, polymerized at 1.8 V, coupling occurs almost exclusively at the α-position. The $(\beta+\beta')/\beta''$ ratio vs the growth potential range is plotted in *Figure 9*. It ranges between 0.01 and 0.14. For any assumed d.p., one can estimate the extent of mislinking, or vice versa. Regardless of the assumed per cent of mislinks, the d.p. generally decreases

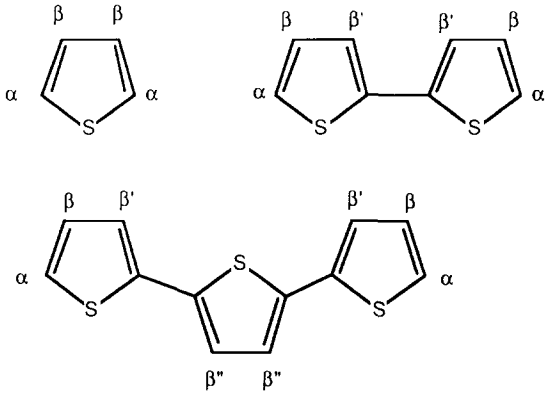

Figure 7 Designation of the β hydrogen sets on thiophene oligomers

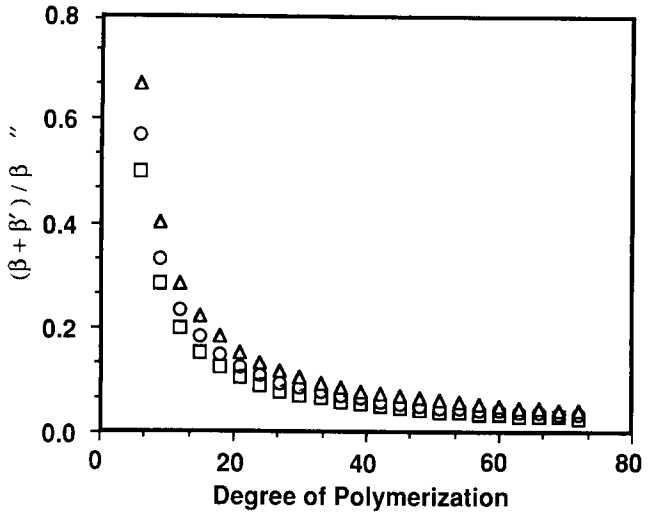

Figure 8 Calculated ratio of β-hydrogens on end groups, $(\beta+\beta')$, to those on internal rings, β'', as a function of the degree of polymerization for three assumed modes of ring linkage: □, 100% α-linked; ○, 50% α-linked; △, 100% β-linked

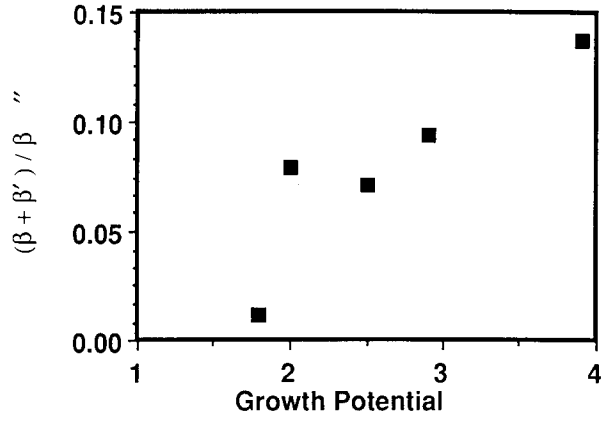

Figure 9 The ratio of $(\beta+\beta')$ hydrogens to the β'' hydrogens (as designated in *Figure 7*) *versus* the growth potential for poly(SSS) films

with increasing growth potential. The implied increase in β-coupling with growth potential parallels that observed for thiophene and α-bithienyl electropolymerizations[28].

Voltammetry of poly(SXS) films

Cyclic voltammograms for the SXS polymers deposited on Pt microelectrodes display quasi-reversible redox behaviour. A representative experiment is shown in *Figure 10* for poly(SOS). The peak anodic potentials shift approximately linearly with scan rate up to 200 mV/s. We have taken the extrapolated peak potentials at zero scan-rate as the energy from which to compare the oxidation potentials of the different SXS polymers and have arbitrarily assigned it to the top of the valence band. This is only a crude approximation, however, because several factors (such as heterogeneous electron transfer kinetics, uncompensated resistance, porosity of the films and hence mobility of counterions) contributing to different degrees, combine to cause the peak shifts and we have not assessed their relative importance.

Peak anodic (i_{pa}) and cathodic (i_{pc}) currents are directly proportional to $v^{1/2}$ for all four polymer systems (see *Figure 11*). The ratio of i_{pa}/i_{pc} is less than unity in each case, suggesting that some structural changes accompany the redox process. A change from a twisted conformation for the neutral polymer to one which is more planar for the charged (oxidized) polymer has been inferred from the voltammetric behaviour of polythiophene made from oligomers of different lengths[28]. It seems reasonable to assume that a similar mechanism is operating for the alloys.

Table 2 compares the peak oxidation potentials and long wavelength absorbance for the SXS monomers and polymers. The former is related to the HOMO (or upper valence band) energy; the latter to the HOMO-LUMO separation (or band gap).

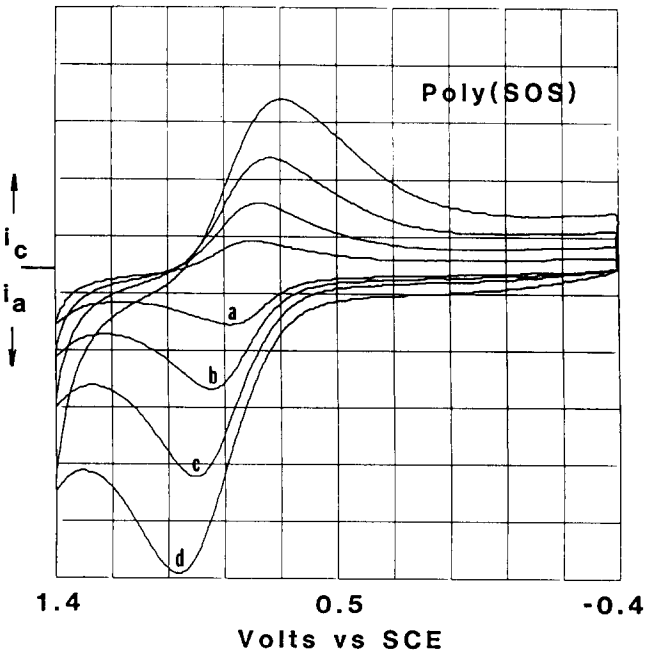

Figure 10 Cyclic voltammograms for a poly(SOS) film deposited on a Pt microelectrode as a function of scan rate. (a) 40 mV s^{-1}; (b) 100 mV s^{-1}; (c) 200 mV s^{-1}; (d) 400 mV s^{-1}

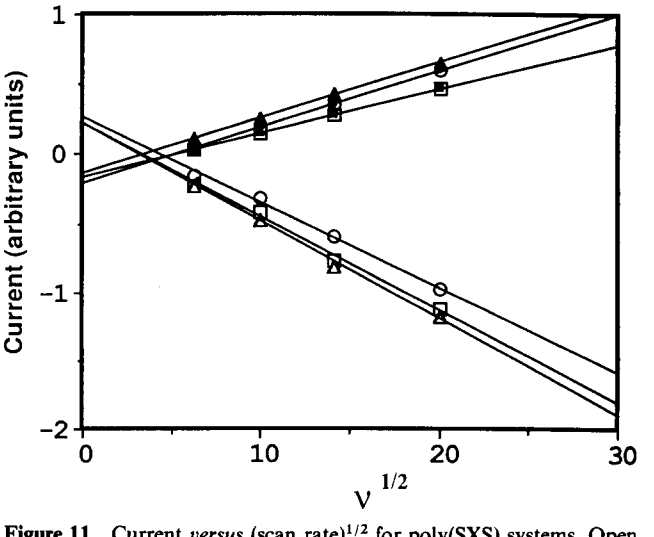

Figure 11 Current *versus* (scan rate)$^{1/2}$ for poly(SXS) systems. Open and closed symbols represent peak anodic and peak cathodic currents, respectively. □, SSS; △, SOS; ○, SNS

Table 2 Long wavelength absorbance and peak anodic potentials for SXS systems

	Monomers		Polymers	
System	$h\nu_{min}$ (eV)	E_{pa} (V)[a]	$h\nu_{min}$ (eV)	E_{pa} (V)[a]
SNS	3.65	0.66	2.77	0.59–0.61
SMS	3.89	0.74	2.96	0.94–0.98
SOS	3.55	0.94	2.61	0.81–0.83
SSS	3.53	1.01	2.70	0.88–0.91

[a] Potentials *versus* SCE, corrected using Ferrocene as internal standard

Table 3 Electrical conductivities of poly(SXS) films

Monomer	Conductivity (S/cm)
SSS	20
SOS	0.3
SNS	280
SMS	1
S	>100[1]
N	>100[1]
O	80[1]
N–CH_3	<0.001[1]

D.c. electrical conductivity of SXS films

Films of the SXS polymers held overnight at their maximum reversible doping potential attain high doping levels. These were removed from the electrode with plastic tape and the four-probe d.c. conductivity was determined at room temperature (*Table 3* summarizes the results). The poly(SSS) films are within a factor of 5 of what others have observed for polythiophene. Poly(SNS) exhibits the highest conductivity of the alloys, whereas poly(SMS) is two orders of magnitude less conductive. This should be compared to the 5–6 order of magnitude difference[1] between comparably doped polypyrrole, *N*, and poly(*N*-methyl-pyrrole), *N*–CH_3. Steric interactions between the methyl hydrogens and the adjacent rings in poly(*N*-methylpyrrole) prevent the rings from achieving coplanarity in the oxidized state. Evidently these constraints are relaxed to some degree on the SMS polymer, where only every third ring has a methyl substituent on the nitrogen. Analogous steric problems are absent for poly(SOS), however, so its low conductivity may reflect a less ordered system.

It is well known that the various heteroaromatics have different oxidation potentials and display varying degrees of aromaticity[29]. These differences should be reflected in the ease and degree of polymerization of the monomers and the electronic properties of the polymer. The band gap of the neutral homopolymers clearly varies with the heteroatom. The results of numerous studies on these and related systems show that the characteristics of the resultant polymers derive from a complicated interplay of solvent, electrolyte and monomer concentration in the growth medium and these vary with the different monomers. Monomers which oxidize at high potentials, yielding radical ions which are very unstable, do not readily polymerize[31], preferring nucleophilic substitution reactions with solvent or electrolyte. Substrates that furnish very stable ion radicals may also be reluctant toward polymerization, affording soluble oligomers instead[32]. The nature of the heteroatom is one factor that must be considered.

The two extreme views of the poly(heteroaromatics) treat the heteroatom as either a minor perturbation to or as the determining factor in the π-system. In the former, the heteroatom serves mostly to hold the carbon framework of a polyacetylene in a rigid configuration and its nature contributes little to the transport properties of the materials[33,34]. The similarities in the magnitudes of the electrical conductivity for highly doped polythiophene, polypyrrole and polyfuran, and the identical *g*-shifts for lightly to moderately doped polythiophene and polypyrrole[35,36] as well as their similarity to AsF_5-doped polyacetylene[37] is taken as evidence for the secondary role of the heteroatom. The latter view is exemplified by the theoretical work by Mintmire *et al.*[38] which demonstrates that the dominant interaction occurs between the *p*-orbital lone pair electrons of the heteroatom and the π-band structure of the carbon backbone, with only minor effects on the σ-structure. HMO calculations on homo- and copolymers of furan, pyrrole and thiophene[39] imply that the band gaps may be varied by altering the heteroatom composition. Calculations have shown that the band gap decreases linearly with the amount of quinoid structure the polymer chain can assume upon doping[40], and the energy required to attain this configuration varies with the structure of the aromatic moiety (20.1, 16.1 and 14.4 kcal/mol per ring for benzene, thiophene and pyrrole, respectively). The heteroatom affords then an important degree of freedom in the design and control of the electronic and (perhaps more significantly) the mechanical properties of the polymers. Furthermore, in as much as it contributes to the ease of oxidation of the heteroaromatic, the stability of the resultant ion radical and the charge/spin distribution within this species, the nature of the heteroatom is an important determinant in the structures of the polymers obtained.

One may construct a qualitative picture of the energy level diagram for the various SXS polymers from the *in situ* doping studies and their cyclic voltammetry. The band gap is taken as the point of zero crossing of the *x*-axis in the difference absorption spectra. The levels of the bipolaron states are taken as the maxima in lightly oxidized polymers. These shift as the polymers are further oxidized. In order to compare one alloy to another, we have chosen the electrochemical E_{pa} as defining the HOMO (or valence band) energy level, but admit to some ambiguity in its determination. *Figure 12* presents the derived energy level diagram for the polymers. The indicated bandwidths are arbitrary. As the heteroatom composition is changed, we observe differences in the band gaps, the ionization potentials, and the symmetry of the placement of the mid-gap states.

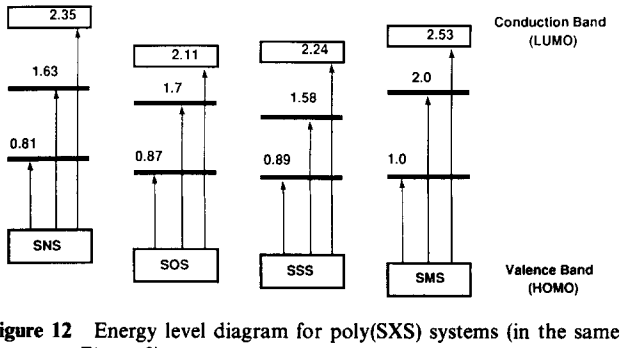

Figure 12 Energy level diagram for poly(SXS) systems (in the same format as *Figure 3*)

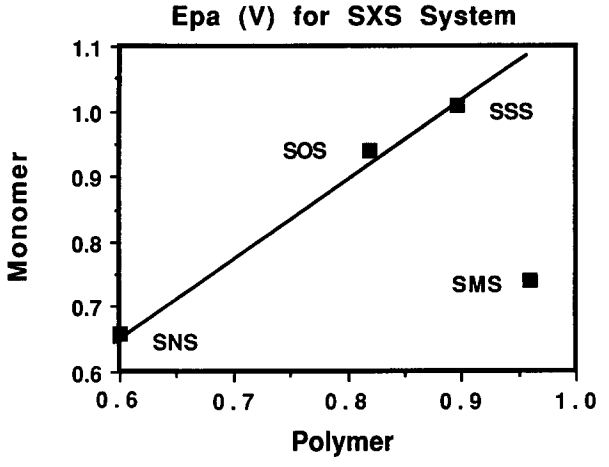

Figure 13 Peak anodic potentials (vs SCE) of SXS monomers *versus* SXS polymers

Substitution by methyl or ethyl at the 3-position in thiophene changes the optical absorption spectra of the resulting polymers[41]. The band gaps of neutral poly(3-methylthiophene) (PMT) and poly(3-ethylthiophene) (PET) are respectively smaller and larger than that of polythiophene. When doped, however, the spectra of PMT and PET are very similar. The implication is that the substituents' electronic and steric effects compete in the neutral state, where they respectively lower the oxidation potential of the monomer (due to electron release), or, depending on their size, raise it by forcing successive thiophene rings out of coplanarity. In the doped state, where the rings once again achieve a coplanar arrangement(!), the electronic effect dominates. This is to be contrasted with poly(SNS) and poly(SMS), where only steric effects seem to be important. Methyl substitution on the nitrogen of pyrrole has no effect on the oxidation potential, because the coefficient of the HOMO is zero at that site. Similarly, *N*-methyl substitution on SNS to afford SMS should also have a minimal effect on the oxidation potentials, yet SMS is harder to oxidize by ca 100 mV. The difference in $h\nu_{min}$ between SNS and SMS monomers (0.24eV) and the corresponding band gap difference for the polymers (0.18 eV) also show that methyl substitution affects these energy levels. The difference in E_{pa}s for the polymers (0.36 V) is even greater than for the monomers (0.08 V). In as much as the E_{pa} may be related to the HOMO level, it appears that the methyl group has its greatest effect here. The moderate conductivity of oxidized poly(SMS) suggests that the quinoidal phase can still achieve some degree of planarity. When steric effects are secondary, a good correlation exists between the oxidation potential of the monomer and that of the polymer (*Figure 13*).

CONCLUSIONS

The optical and electrical properties of poly(heteroaromatics) depend, in part, on the heteroatom composition. Variation in this composition through copolymers affords a powerful means to control the properties of these materials. Similarities in the oxidation potentials of the monomers facilitates the production of copolymers and the SXS monomers offer a range of potentials (ca 400 mV) over which combinations of monomers may be copolymerized. The heteroatom composition affects the electronic characteristics of the monomers and polymers but is not the sole determinant of their properties because, in some cases, steric factors may be more important. These seem to be particularly significant in the case of poly(*N*-substituted pyrrole) homopolymers where they effectively prevent the quinoidal phase from achieving coplanarity. These steric factors are relaxed for *N*-substituted SNS derivatives, however, because the adjacent thiophene rings act as steric diluents. Nevertheless, caution must be exercised in selecting and positioning the substituent.

ACKNOWLEDGEMENTS

It is a pleasure to acknowledge the many helpful discussions with Dr Wayne E. Britton, and the programming efforts of Mr Joseph E. Preston which greatly facilitated data acquisition and reduction. The generous provision of ITO electrodes by Dr Jacob Lin of Polytronix, Inc. is greatly appreciated.

REFERENCES

1 Skotheim, T. E. (Ed.) 'Handbook of Conductive Polymers', Marcel Dekker, New York, (1986)
2 Tsumura, A., Koezuka, H., Tsunoda, S., Ando, T. *Chem. Lett.* 1986, 863
3 Kaneto, K., Maxfield, M., Nairns, D. P., MacDiarmid, A. G. and Heeger, A. J. *J. Chem. Soc. Faraday Trans. I* 1982, **78**, 3417
4 Horowitz, G. and Garnier, F. *Solar Energy Materials* 1986, **13**, 47
5 Horowitz, G. *Ann. Physique* 1986, **11**, 31
6 Aizawa, M., Yamada, T., Shinohara, H., Akagi, K. and Shirakawa, H. *J. Chem. Soc. Chem. Commun.* 1986, 1315
7 Kaneko, M., Yamada, A., Kenmochi, T. and Tsuchida, E. *J. Polym. Sci., Polym. Lett. Edn.* 1985, **23**, 629
8 White, H. S., Kittlesen, G. P. and Wrighton, M. S. *J. Am. Chem. Soc.* 1984, **106**, 5375
9 DePaoli, M., Waltman, R. J., Diaz, A. F. and Bargon, J. *J. Chem. Soc. Chem. Commun.* 1984, 1015
10 Wang, T. T., Tasaka, S., Hutton, R. S. and Lu, P. Y. *J. Chem. Soc. Chem. Commun.* 1985, 1343
11 Krische, B. and Ahlgren, G. *Mol. Cryst. Liq. Cryst.* 1985, **121**, 325
12 Bocchi, V. and Gardini, G. *J. Chem. Soc. Chem. Commun.* 1986, 148
13 Penner, R. and Martin, C. R. *J. Electrochem. Soc. Electrochem. Sci. Tech.* 1986, **133**, 310
14 Meyer, W. H., Kiess, H., Binggeli, B., Meier, E. and Harbeke, G. *Synthetic Metals* 1985, **10**, 255
15 Heeger, A. J., Moses, D. and Sinclair, M. *Synthetic Metals* 1986, **15**, 95
16 Ohsawa, T., Kaneto, K. and Yoshino, K. *Japan. J. Appl. Phys.* 1984, **23**, L663
17 Ferraris, J. P. and Skiles, G. D. *Polymer* 1987, **28**, 179
18 Chung, T. C., Kaufman, J. H., Heeger, A. J. and Wudl, F. *Phys. Rev. B* 1984, **30**, 702
19 Bredas, J. L. *Mol. Cryst. Liq. Cryst.* 1985, **118**, 49
20 Bredas, J. L., Scott, J. C., Yahusli, K. and Street, G. B. *Phys. Rev. B* 1984, **30**, 1023
21 Conwell, E. M. *Synthetic Metals* 1985, **11**, 21
22 Koebel, W., Kiess, H., Egli, M. and Keller, R. *Mol. Cryst. Liq. Cryst.* 1986, **137**, 141
23 Tanaka, K., Shichiri, T. and Yamabe, T. *Synthetic Metals* 1986, **14**, 271
24 Ignanas, O., Liedberg, B. and Chang-Ru, W. *Synthetic Metals* 1985, **11**, 249
25 Yumoto, Y. and Yoshimura, S. *Synthetic Metals* 1986, **13**, 185
26 Roncali, J., Garnier, F., Lemaire, M. and Garreau, M. *Synthetic Metals* 1986, **15**, 323
27 Akiyama, M. *J. Mol. Spec.* 1972, **43**, 226

28 Heinze, J., Mortensen, J. and Hinkelmann, K. *Synthetic Metals* 1987, **21**, 209
29 Fringuelli, F., Marino, G., Taticchi, A. and Gandolino, G. *J. Chem. Soc. Perkin Trans.* 1974, **2**, 332
30 Calderbank, K. E., Calvert, R. L., Lukins, P. B. and Ritchie, G. L. D. *Aust. J. Chem.* 1981, **34**, 1835
31 Waltman, R. J., Diaz, A. F. and Bargon, J. *J. Phys. Chem.* 1984, **88**, 4343
32 Dian, G., Barbey, G. and Decroix, B. *Synthetic Metals* 1986, **13**, 281
33 Chung, T. C., Kaufman, J. J., Heeger, A. J. and Wudl, F. *Phys. Rev. B* 1984, **30**, 702
34 Heeger, A. J. *Polym. J.* 1985, **17**, 201
35 Tourillon, G., Gourier, D., Garnier, P. and Vivien, D. *J. Phys. Chem.* 1984, **88**, 1049
36 Ford, W. K., Duke, C. B. and Salanek, W. R. *J. Chem. Phys.* 1982, **77**, 5030
37 Goldberg, I. B., Crowe, H. R., Newman, F. R., Heeger, A. J. and MacDiarmid, A. G. *J. Chem. Phys.* 1979, **70**, 1132
38 Mintmire, J. W., White, C. T. and Elert, M. L. *Synthetic Metals* 1986, **16**, 235
39 Lagerstedt, I. and Wennerstrom, O. *Synthetic Metals* 1987, **20**, 269
40 Bredas, J. L. *Chem. Phys.* 1985, **82**, 3808
41 Sato, M., Tanaka, S. and Kaeriyama, K. *Synthetic Metals* 1986, **14**, 279